

# A Neck Injury Analyzer Tool Based on Mechanical Impedance Characteristics for the Design of Human-seat Systems

Yusaku Takeda \*, Yoshiyuki Tanaka \*, Toshio Tsuji \*,  
Toru Takeshima †, Tetsuro Kusuhara † and Yoshihito Kawashima †

\*Department of Artificial Complex Systems Engineering, Hiroshima University  
4-1 Kagamiyama 1-chome, Higashi-Hiroshima, Hiroshima, 739-8527, Japan  
Tel: +81-82-424-7676, Fax: +81-82-422-7030

Email:takeda@bsys.hiroshima-u.ac.jp, ytanaka@bsys.hiroshima-u.ac.jp and tsuji@bsys.hiroshima-u.ac.jp

†DELTA KOGYO CO.,LTD.

1-14 Futyu-cho, Aki-gun, Hiroshima, 735-8501, Japan  
Tel: +81-82-282-8211, Fax: +81-82-282-8221

**Abstract**—The importance of developing a driving seat effective for reducing neck injuries has been increased to produce a safer automobile against car accidents in recent years. However, there does not exist an efficient methodology to develop such an innovative driving seat with consideration of dynamic characteristics of a human body as well as the interactions between a driver and a seat.

The present paper proposes a new simulation method based on the mechanical impedance properties of a human-seat system that can provide quantitative analysis of neck injuries. Effectiveness of the proposed method is shown through a set of computer simulations by changing dynamic properties of a seat model.

**Keywords**—mechanical impedance; a human-seat system; neck injury

## I. INTRODUCTION

Neck injuries occupy about 45 % of the injuries caused by motor vehicle accidents in Japan [1]. Therefore there has been expected to reduce a whiplash effect in recent years, while the international organization for standardization (ISO) established the general guideline for the car collision test in rear-end impacts at a low speed as well as the standard measurements for evaluating the degree of neck injury. The importance of developing a driving seat effective for reducing neck injuries will be increased further to produce a safer automobile car in the near future.

To cope with such a problem, the study for reducing the whiplash effect have been activity conducted. For example, Svensson et al. [2] examined the mechanism of neck injuries through the experiments with a pig in stead of a human driver, and reported that the change of pressure in the spinal column would be a main factor causing neck injuries. Also, some experimental research works using a living human as well as a cadaver have been presented

by using a quantitative index. Boström et al. [3] proposed the neck injury criteria, so-called NIC, which evaluates the relative acceleration and velocity between the head and the 1st thoracic vertebrae. Schmitt et al. [4] proposed the neck protection criteria, Nkm, which evaluates the shear force and the sagittal bending moment of the neck.

On the other hand, there are several studies that try to reveal the neck injury mechanism by means of computer simulation techniques. Kirkoartik et al. [5] constructed a computer model of a human driver by using LS-DYNA, which is the multi purpose analyzer tool based on a non-linear dynamic finite element method (FEM), and simulated various situations of the car collision. Furusu [6] created a model of the human cervical vertebrae by the FEM model and examined the correlation between the injury to the cervical vertebrae and the shear force along the sagittal axis of the cervical vertebrae. However, there does not exist a research study considering the interactive effects between a human driver and a driving seat in rear-end impacts.

A couple of researches expressed the dynamic characteristics of a driving seat by the mechanical impedance parameters: i.e., stiffness, viscosity, and inertia. Svensson et al. [7] and Nilson [8] produced a prototype seat, in which the headrest and the seatback is devised for reducing neck injuries, and showed that the degree of neck injuries becomes larger as the stiffness of a seatback joint increase through the car collision test in rear-end impacts with a dummy doll. They also pointed out that the force transfer characteristics between a human driver and a seat is important to discuss the mechanism of neck injuries. However, there is no effective method of designing a driving seat considering such dynamic characteristics of a human-seat system.

The goal of this study is to establish a new design method

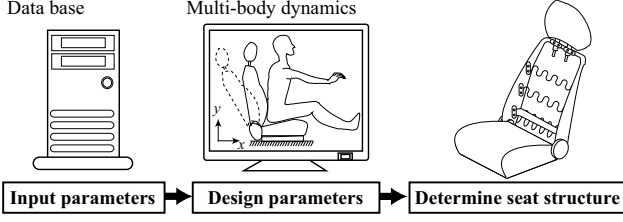


Figure 1. Design process using the simulation tool.

of a driving seat using computer simulations. It can be much expected to shorten the process of manufacturing the driving seats without a trial production and a car collision test. As the first step, this paper develops the prototype analyzer tool to provide a quantitative evaluation to the degree of neck injuries considering the mechanical impedance characteristics of a human-seat system. This paper is organized as follows: Section 2 explains the neck injury analyzer tool based on multi-body dynamics and mechanical impedance. Section 3 performs the simulation of human dynamic behaviors according to the changes of impedance characteristics of a driving seat, and discusses the mechanical impedance of the driving seat for reducing the neck injuries effectively.

## II. THE NECK INJURY ANALYZER TOOL

### A. System structure

Fig. 1 shows the general design process of a driving seat against neck injuries by the proposed analyzer tool.

The developed tool has a database of the physical parameters of a human-seat system; i.e. the stature and weight of a driver; the size and weight of seat parts; and the impedance properties of driver's skin and joints, seat cushioning, and seat joints, which had been measured or estimated in advance. Note that, in this paper, a dummy doll is used instead of a human driver.

This tool can simulate dynamic movements of a human-seat system in rear-end impacts, and can evaluate the degree of neck injuries, such as the NIC, according to the viscoelastic properties of a seat model.

### B. Model

Fig. 2 shows the schematic representation of a human-seat model.

A seat model is expressed by 3 rigid links with rotational joints ( $s_1$ : a joint at the edge of the seat,  $s_2$ : a joint in between cushion-seatback,  $s_3$ : a joint in between seatback-headrest), where the edge of the seat is fixed by the rotational joint on the environment. Its dynamic equation can be written by

$$\mathbf{M}_s \ddot{\mathbf{q}}_s + \mathbf{h}_s(\mathbf{q}_s, \dot{\mathbf{q}}_s) = \mathbf{B}_s \dot{\mathbf{q}}_s + \mathbf{K}_s(\mathbf{q}_s - \mathbf{q}_{v_s}) + \boldsymbol{\tau}_{ext_s} \quad (1)$$

where  $\mathbf{q}_s, \mathbf{q}_{v_s} \in \mathbb{R}^3$  represent the joint angle vector of the seat model and the virtual equilibrium point in the joint level, respectively;  $\mathbf{M}_s, \mathbf{B}_s, \mathbf{K}_s \in \mathbb{R}^{3 \times 3}$  the joint inertia, viscosity, and stiffness matrices;  $\mathbf{h}_s(\mathbf{q}_s, \dot{\mathbf{q}}_s) \in \mathbb{R}^3$  the term

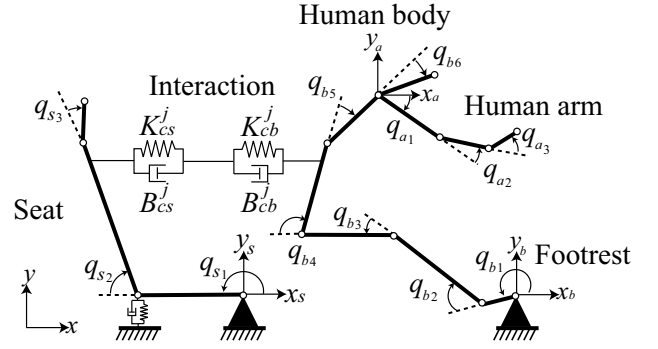


Figure 2. A schematic representation of a human-seat.

with respects to centrifugal, coriolis, and gravity force; and  $\boldsymbol{\tau}_{ext_s} \in \mathbb{R}^3$  the external joint torque.

A human model is expressed by 9 rigid links with 9 DOFs, in which the upper arm has 3 rotational joints ( $a_1$ : the shoulder joint,  $a_2$ : the elbow joint,  $a_3$ : the wrist joint), while the body including the leg part has 6 rotational joints ( $b_1$ : tip of a toe,  $b_2$ : the ankle joint,  $b_3$ : the knee joint,  $b_4$ : the hip joint,  $b_5$ : the 12th thoracic vertebrae joint,  $b_6$ : the 1st thoracic vertebrae joint). The tip of a toe is fixed by the rotational joint on environment under assumption that the tip of a toe is constrained by the footrest. The dynamics of a whole human body can be then given by

$$\begin{bmatrix} \mathbf{M}_a & 0 \\ 0 & \mathbf{M}_b \end{bmatrix} \begin{bmatrix} \ddot{\mathbf{q}}_a \\ \ddot{\mathbf{q}}_b \end{bmatrix} + \begin{bmatrix} \mathbf{h}_a(\mathbf{q}_a, \dot{\mathbf{q}}_a) \\ \mathbf{h}_b(\mathbf{q}_b, \dot{\mathbf{q}}_b) \end{bmatrix} = \begin{bmatrix} \mathbf{B}_a & 0 \\ 0 & \mathbf{B}_b \end{bmatrix} \begin{bmatrix} \dot{\mathbf{q}}_a \\ \dot{\mathbf{q}}_b \end{bmatrix} + \begin{bmatrix} \mathbf{K}_a & 0 \\ 0 & \mathbf{K}_b \end{bmatrix} \begin{bmatrix} \mathbf{q}_a - \mathbf{q}_{v_a} \\ \mathbf{q}_b - \mathbf{q}_{v_b} \end{bmatrix} + \begin{bmatrix} \boldsymbol{\tau}_{ba} \\ \boldsymbol{\tau}_{ab} \end{bmatrix} + \begin{bmatrix} 0 \\ \boldsymbol{\tau}_{ext_b} \end{bmatrix}, \quad (2)$$

with the following constraint condition between the shoulder joint and the 1st thoracic vertebrae as

$$\ddot{\mathbf{x}}_{\xi_a} - \ddot{\mathbf{x}}_{b_6} = 0, \quad (3)$$

where  $\mathbf{q}_a \in \mathbb{R}^3$  and  $\mathbf{q}_b \in \mathbb{R}^6$  represent the joint angle vector of the upper arm and the body, respectively;  $\mathbf{q}_{v_a} \in \mathbb{R}^3$  and  $\mathbf{q}_{v_b} \in \mathbb{R}^6$  the virtual equilibrium points in the joint level of the upper arm and body;  $\mathbf{M}_a, \mathbf{B}_a, \mathbf{K}_a \in \mathbb{R}^{3 \times 3}$  the joint inertia, viscosity, and stiffness matrices of the upper arm;  $\mathbf{M}_b, \mathbf{B}_b, \mathbf{K}_b \in \mathbb{R}^{6 \times 6}$  impedance matrices of the body;  $\mathbf{h}_a(\mathbf{q}_a, \dot{\mathbf{q}}_a) \in \mathbb{R}^3$  and  $\mathbf{h}_b(\mathbf{q}_b, \dot{\mathbf{q}}_b) \in \mathbb{R}^6$  the terms with respects to centrifugal, coriolis, and gravity force of the arm and body;  $\boldsymbol{\tau}_{ba} \in \mathbb{R}^3$  the external force which is transferred from the body to upper arm;  $\boldsymbol{\tau}_{ab} \in \mathbb{R}^6$  the external force which is transferred from the upper arm to body;  $\boldsymbol{\tau}_{ext_b} \in \mathbb{R}^6$  the external joint torque of upper arm and body;  $\ddot{\mathbf{x}}_{\xi_a} \in \mathbb{R}^2$  the translational acceleration of the shoulder  $a_1$ ;  $\ddot{\mathbf{x}}_{b_6} \in \mathbb{R}^2$  the translational acceleration of the 1st thoracic vertebrae  $b_6$  which is calculated by joint angle vector  $\ddot{\mathbf{q}}_b$ .

As shown in Fig. 3, an interactive force  $\mathbf{F}_{int_b}^j \in \mathbb{R}^2$  at the contact point between the position vectors of the virtual contact points on the seat/human's rigid links  $\mathbf{x}_{cs}^j$ ,

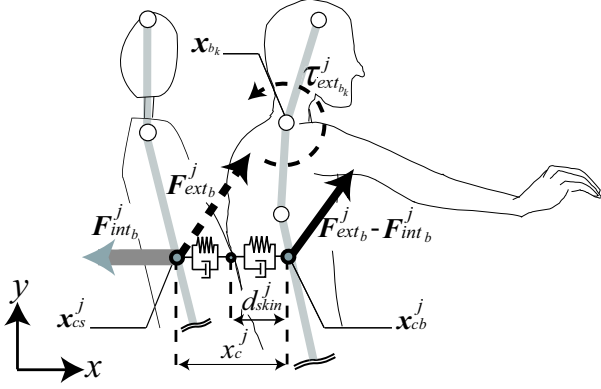


Figure 3. Interactive force transferring to human body.

$x_{cb}^j \in \mathbb{R}^2$  is expressed as follows:

$$\mathbf{F}_{int_b}^j = [F_{int_b}^j, 0]^T, \quad (4)$$

$$F_{int_b}^j = \begin{cases} B_{cs}^j \dot{x}_c^j + K_{cs}^j (x_c^j - x_{cv}^j) & (x_c^j - x_{cv}^j < -d_{skin}^j) \\ \left( \frac{B_{cs}^j B_{cb}^j}{B_{cs}^j + B_{cb}^j} \right) \dot{x}_c^j + \left( \frac{K_{cs}^j K_{cb}^j}{K_{cs}^j + K_{cb}^j} \right) (x_c^j - x_{cv}^j) & (-d_{skin}^j \leq x_c^j - x_{cv}^j \leq 0) \\ 0 & (x_c^j - x_{cv}^j > 0), \end{cases} \quad (5)$$

where the subscript  $j$  indicates the contact point  $j$ ;  $B_{cs}^j, K_{cs}^j \in \mathbb{R}^1$  the surface viscosity and stiffness of the seat;  $B_{cb}^j, K_{cb}^j \in \mathbb{R}^1$  the surface viscosity and stiffness of the human body at the contact point  $j$ ;  $x_c^j \in \mathbb{R}^1$  ( $= |x_{cb}^j - x_{cs}^j|$ ) the distance between the human to seat's rigid links; and  $x_{cv}^j$  the equilibrium position on  $x_c^j$ ;  $d_{skin}^j \in \mathbb{R}^1$  the thickness of the skin.

The external force to a human joint  $\mathbf{F}_{ext_b}^j \in \mathbb{R}^2$  is generated by the seat link at the position vector  $\mathbf{x}_{cs}^j$  as shown in Fig. 3. The external torque to the  $k$ -th human joint  $\tau_{ext_b_k}^j$ , which works to the joint  $b_k$ , is expressed as

$$\tau_{ext_b_k}^j = (\mathbf{F}_{ext_b}^j - \mathbf{F}_{int_b}^j) \times (\mathbf{x}_{b_k} - \mathbf{x}_{cb}^j), \quad (6)$$

where  $\mathbf{x}_{b_k} \in \mathbb{R}^2$  ( $k = 1 \dots 7$ ) represent the position vector of the joint  $b_k$  of a human body. The dynamic motion simulation of a human-seat system is performed on the basis of the multi-body dynamics as mentioned above.

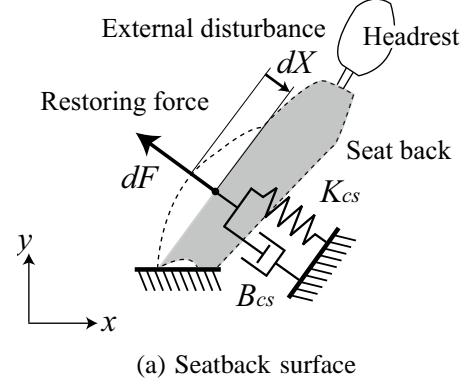
### C. Estimation of the seat impedance properties

The database has the measured mechanical impedance characteristics of a real seat surface and joint as well as the physical parameters of a dummy doll (BioRID-II, Denton ATD, Inc.).

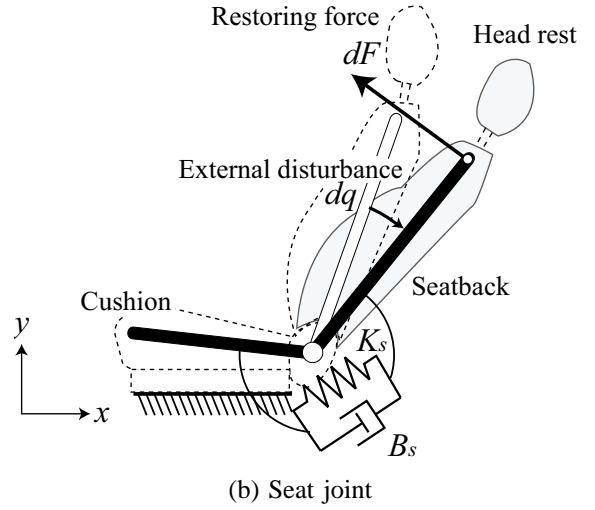
The mechanical impedance model of a driving seat surface are expressed by the impedance parameters as follows:

$$B_{cs} d\dot{X}(t) + K_{cs} dX(t) = dF(t), \quad (7)$$

where  $dX(t)$ ,  $dF(t) \in \mathbb{R}^1$  denote the displacement of a seat surface and the restoring force from onset time  $t_0$ , respectively;  $B_{cs}, K_{cs} \in \mathbb{R}^1$  represent the viscosity and stiffness of the surface that might be estimated by



(a) Seatback surface



(b) Seat joint

Figure 4. Estimation of the seat impedance.

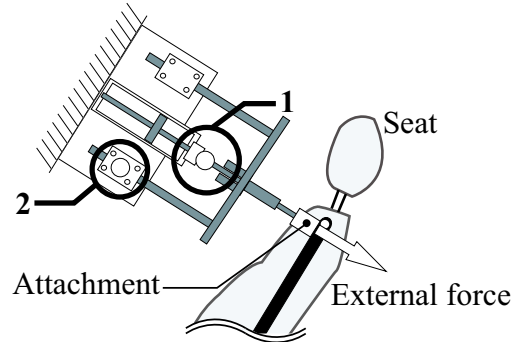


Figure 5. Measurement of the seat impedance.

means of the least squares method with the motion of a seat surface. An external disturbance to the seat surface is applied toward the normal direction as shown in Fig. 4(a), while the impedance parameters of seat joint  $B_s, K_s$  are estimated by the impedance model in the joint level along the similar procedure as shown in Fig. 4(b).

Fig. 5 depicts the experimental apparatus for measuring seat impedance parameters, which consists of the air cylinder and the measurement part of displacement and force. The measurement part is attached at the base of

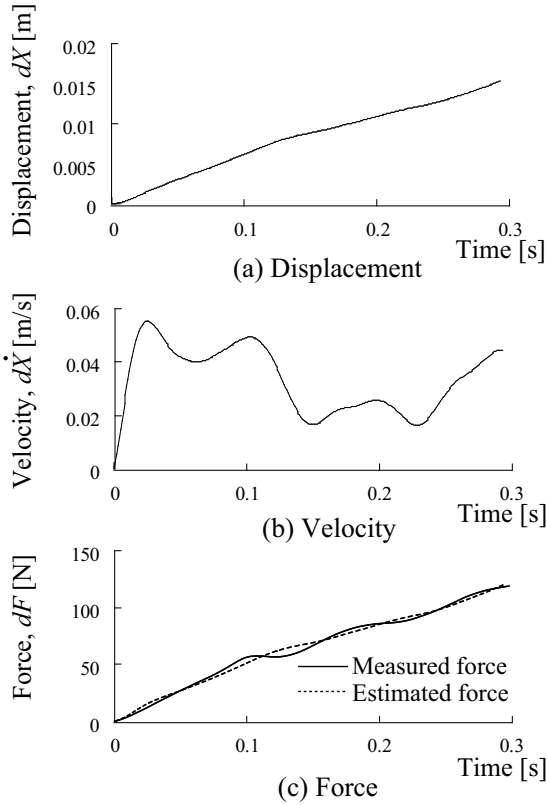


Figure 6. An example of measured signals for measurements of seatback surface impedance.

TABLE I  
EXAMPLE OF IMPEDANCE PARAMETERS ON THE SEATBACK AND JOINT.

Seatback surface	$B_{cs}$ [Ns/m]	$K_{cs}$ [N/m]
	$65.05 \pm 20.45$	$7578.02 \pm 198.45$
Seatback-cushion joint	$B_{s_2}$ [Nms/rad]	$K_{s_2}$ [Nm/rad]
	$142.00 \pm 21.01$	$7175.56 \pm 212.23$

the air cylinder as shown in the black circle 1 and 2. The air cylinder can give the external disturbance to seatback surface and joint by assembling the attachments as shown in Fig. 5. The sampling rate for force and displacement was set at 1 [kHz] in measuring experiments.

Fig. 6 shows an example of the measured signals for estimating impedance of a seat surface, where time histories of surface displacement  $dX(t)$ , surface velocity  $d\dot{X}(t)$ , and measured force  $dF(t)$  are given in the order from top. The time history of the force  $dF(t)$  (solid lines) well agrees with the estimated force (broken lines) computed by (7) using the measured seatback impedance.

Table I shows the measured impedance parameters of the seatback surface and the joint  $s_2$ . Mean values and SDs for 3 sets of estimated results are shown. In this paper, the dynamic motion of a human-seat system is computed with these mechanical impedance parameters.

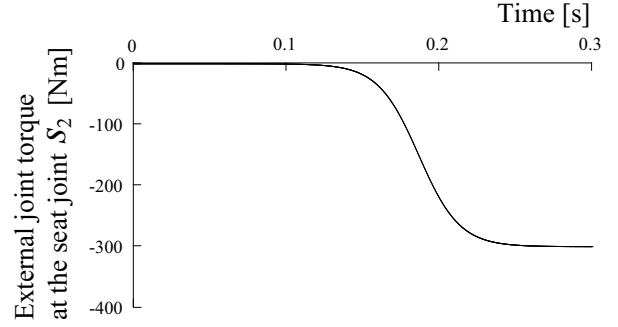


Figure 7. Example of the external joint torque at the seat joint  $s_2$ .

TABLE II  
THE PHYSICAL PARAMETERS OF THE HUMAN-SEAT SYSTEM MODEL.

		Length [m]	Mass [kg]	Inertia [kgm <sup>2</sup> ]
Seat model	Link 1	0.530	5.565	0.1393
	Link 2	0.670	7.035	0.2746
	Link 3	0.210	0.796	0.0037
Human arm	Link 1	0.283	2.00	0.0138
	Link 2	0.251	1.47	0.0080
	Link 3	0.095	0.80	0.0008
Human body	Link 1	0.226	1.25	0.0058
	Link 2	0.351	4.20	0.0454
	Link 3	0.296	6.00	0.0510
	Link 4	0.419	28.26	0.4664
	Link 5	0.188	13.60	0.0656
	Link 6	0.229	4.55	0.0351

### III. COMPUTER SIMULATION EXPERIMENTS

This section demonstrates the computer simulation of human body movements in rear-end impacts according to the changes of impedance characteristics of a driving seat.

#### A. Experimental conditions

The simulations were carried out under the following three conditions;

- I.  $K_{cs} = 7578.02$  [N/m],  $B_{s_2} = 142.00$  [Nms/rad],
- II.  $K_{cs} = 2000.00$  [N/m],  $B_{s_2} = 142.00$  [Nms/rad],
- III.  $K_{cs} = 7578.02$  [N/m],  $B_{s_2} = 500.00$  [Nms/rad].

where the impedance parameters of the seatback surface and the seat joint  $s_2$  of the condition I were defined based on the measured parameters in Table I. The stiffness and viscosity of human skin was set as  $K_{cb} = 366.00$  [N/m] and  $B_{cb} = 1.23$  [Ns<sup>2</sup>/m] [9]. The contact point between a human and a seat was set at the point between the 3th link of the human model and the 2nd link of the seat model, and the human body is constrained by two seatbelts which were set in vertical direction ( $x = 1.8$  [m]) and horizontal direction ( $y = 0.3$  [m]). The skin of the human body was assumed as  $d_{skin}^j = 0.005$  [m]. In the simulation, a step-like external torque as shown in Fig. 7 was exerted on the seat joint  $s_2$ . Table II shows the link parameters of the human-seat system used in the simulations. The viscoelastic properties of a seatbelt, other seat joints and a human body were defined by trial and error. The sampling time for dynamic

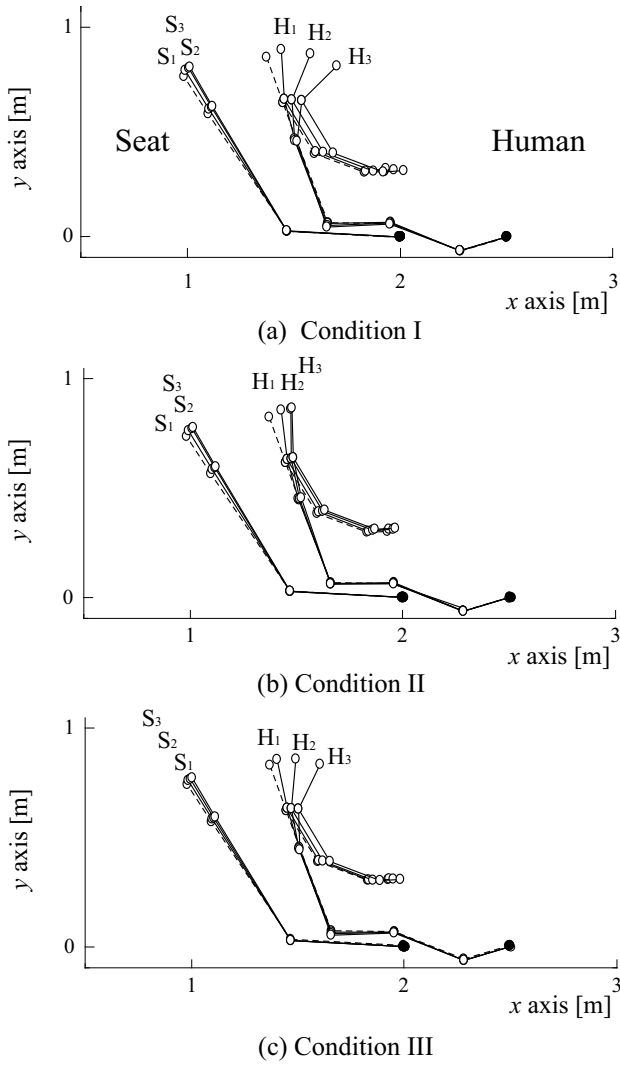


Figure 8. Examples of the simulated dynamic behaviors of the human-seat system.

calculation was at 0.0002 [s], and the onset time of the external torque at 0.02 [s].

### B. Simulation results

Fig. 8 shows the examples of simulated results for each condition. The broken line represents the initial posture of the human and the seat model, while the solid line represents the postures at 0.15, 0.20, 0.30 [s]. The white and the black circle represent the joint and the fixed end of a human-seat system, respectively. It should be noticed that the human model and the seat model in the initial posture are contacted by the skin and the cushioning. In this figure, the 12th thoracic joint  $b_5$  is not pushed out excessively when the stiffness of the seat surface is smaller and the viscosity of the seat joint is larger. The 1st thoracic joint  $b_6$  is bended forward further when the viscosity of the seat joint is smaller. These results may predict that the 1th thoracic joint is given a large torque between 0.20 and 0.30 [s] on the 1st and 3rd conditions.

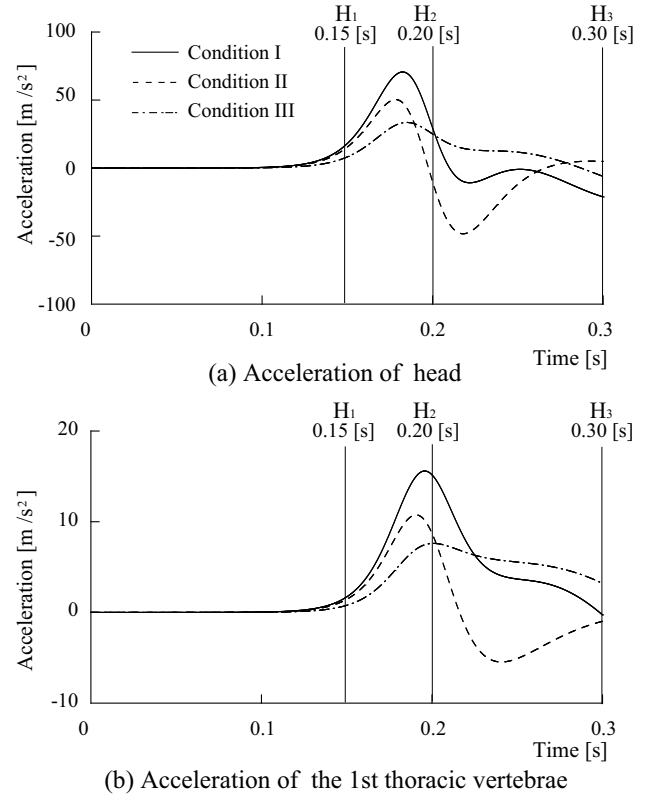


Figure 9. Computed acceleration from the simulated results in Fig. 8.

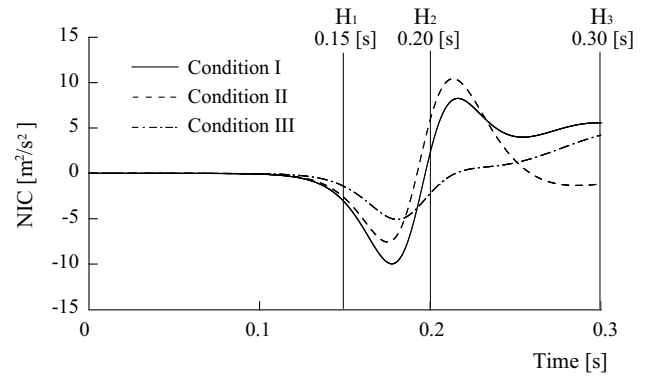


Figure 10. Computed NIC values from the simulated results in Fig. 8.

Fig. 9 shows the acceleration of the head and the 1st thoracic vertebrae. It can be found that the acceleration of the head is much larger than one of the 1st thoracic vertebrae, and becomes very large just after the onset time of the external torque. These results show that a large load is exerted on the neck between 0.15 and 0.30 [s].

Then, the time histories of the NIC value for all of three different conditions were investigated, where the NIC value is calculated as [3]:

$$NIC(t) = 0.2a_{rel}(t) + (v_{rel}(t))^2, \quad (8)$$

$$a_{rel}(t) = a_{T_1}(t) - a_{head}(t), \quad (9)$$

$$v_{rel}(t) = v_{T_1}(t) - v_{head}(t), \quad (10)$$

where  $a_{T_1}(t)$  and  $a_{head}(t)$  represent the acceleration of the

1st thoracic vertebrae and the head in the  $x$  direction;  $v_{T_1}(t)$  and  $v_{head}(t)$  the velocity of the 1st thoracic vertebrae and the head in the  $x$  direction;  $a_{rel}(t)$  and  $v_{rel}(t)$  the relative acceleration and velocity between the 1st thoracic vertebrae and the head. As the larger load is inflicted on the neck, the NIC value is increased.

Fig. 10 shows time profiles according to the specified conditions. The NIC value tends to be large just after the onset of external torque. As the stiffness of the seat surface decreases, the NIC value tends to decrease between 0.15 and 0.20 [s]. While, the NIC value tends to decrease, as the viscosity of the seat joint increases. The viscoelastic properties of the seat surface and joint must be designed carefully in order to develop an effective seat for the reduction of neck injuries.

Thus, the developed tool can evaluate neck injuries with the NIC value according to changes of various viscoelastic parameters of a human-seat model, although the comparison between the results of experiments and simulation and the improvement of this model have to be necessary.

#### IV. CONCLUSION

The present paper has proposed a new design simulation based on the mechanical impedance properties of a human-seat system that can provide quantitative analysis of neck injuries. Then, the dynamic movements of the human-seat system have been computed with respect to the different mechanical impedance properties of the seat by the developed tool. The simulation results showed that the mechanical impedance of the seat joint is one of the important factor to reduce neck injuries. Since the mechanical impedance of a driving seat can be regulated easily in the computer simulations, it can be expected that an effective seat for reduction of neck injuries may be developed by combining the optimization methods with the proposed methods.

Future research will be directed to modify the human-seat model and perform the comparison between experimental and simulated results by using the measured impedance parameters of the whole parts of a driving seat. Then, a driving seat could be designed using the parameters obtained in various simulations by using the proposed methods.

#### ACKNOWLEDGMENT

This research was supported by Grant-in-Aid for Scientific Research of Japan Society for the Promotion of Science (15008210).

#### REFERENCES

- [1] The General Insurance Association of Japan, "The actual condition of traffic accidents of seeing to automobile insurance data (April 2001 ~ March 2002)," 2003 (in Japanese).
- [2] M.Y.Svensson, B.Aldman, P.Lövsund, H.A.Hansson, A Sunesson, T Seeman, and T.Örtengren, "Pressure effects in the spinal canal during whiplash extension motion - a possible cause of injury to the cervical spinal ganglia," Proceedings of International IRCOBI Conference on the Biomechanics of Impact, pp. 189-200, 1993.
- [3] O.Boström, M.Y.Svensson, B.Aldman, H.A.Hansson, Y.Haland, P.Lövsund, T.Seeman, A.Suneson, A. Säljö, and T.Örtengren, "A new neck injury criterion candidate-based on injury findings in the cervical spinal ganglia after experimental sagittal whiplash," Proceedings of International IRCOBI Conference on the Biomechanics of Impact, pp. 123-136, 1996.
- [4] K.-U.Schmitt, M.H.Muser, and P.Niederer, "A new neck injury criterion candidate for rear-end collisions taking into account shear forces and bending moments," Proceedings of ESV: 17th International Technical Conference on the Enhanced Safety of Vehicles (CD-ROM), Report No.184, 95752 B74, 2001.
- [5] S.W.Kirkpartik, R.MacNeill, and R.T.Bocchieri, "Development of an LS-DYNA occupant model for use in crash analyses of roadside safety features," Proceedings of 82nd Annual Meeting of the Transportation Research Board (CD-ROM), Paper No. 03-4450, 2003.
- [6] K.Furusu, "Analysis of injury of human cervical spine using finite element method," The R & D Review of Toyota CRDL, Vol.33, No.1, pp. 53-61, 1998 (in Japanese).
- [7] M.Y.Svensson, P.Lövsund, Y.Haland, and S.Larsson, "The influence of seat-back and head-restraint properties on the head-neck motion during rear-impact," Proceedings of International IRCOBI Conference on the Biomechanics of Impact, pp. 395-406, 1993.
- [8] G.Nilson, "Effects of seat and seat-belt design on car occupant response in frontal and rear impacts," Doctoral thesis, Dept. of Injury Prevention, Chalmers Univ. of Techn., S-412 96 Göteborg, Sweden, 1994.
- [9] T.Irie, H.Oka, and T.Yamamoto, "Measurement of biomechanical properties on skin by impact response," IEICE Transactions on Information and Systems D-II, Vol.75, No.4, pp. 799-807, 1992 (in Japanese).
- [10] M.R.Cutkosky and I.Kao, "Computing and controlling the compliance of a robotic hand," IEEE Transactions on Robotics and Automation, Vol.5, No.2, pp. 151-165, 1989.